

An Energy-efficient Flexible Multi-modal Wireless Sweat Sensing System Based on Laser Induced Graphene

Supplementary Materials

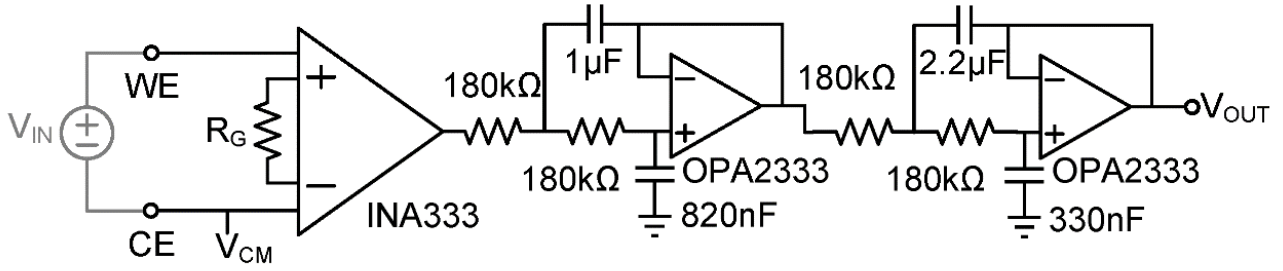
Jiuqing Feng¹, Yizhou Jiang¹, Kai Wang¹, Jianzheng Li¹, Jialong Zhang¹, Mi Tian², Guoping Chen^{1,*},
Laigui Hu¹, Yiqiang Zhan¹ and Yajie Qin^{1,*}

¹ School of Information Science and Technology, Fudan University, Shanghai, 200433, China

² Huashan Hospital, Shanghai 200040, China

*Corresponding author. Email: yajieqin@fudan.edu.cn (Y.Q.); gpchenapple@fudan.edu.cn (G.C.)

(a) Voltage Channel



(b) Current Channel

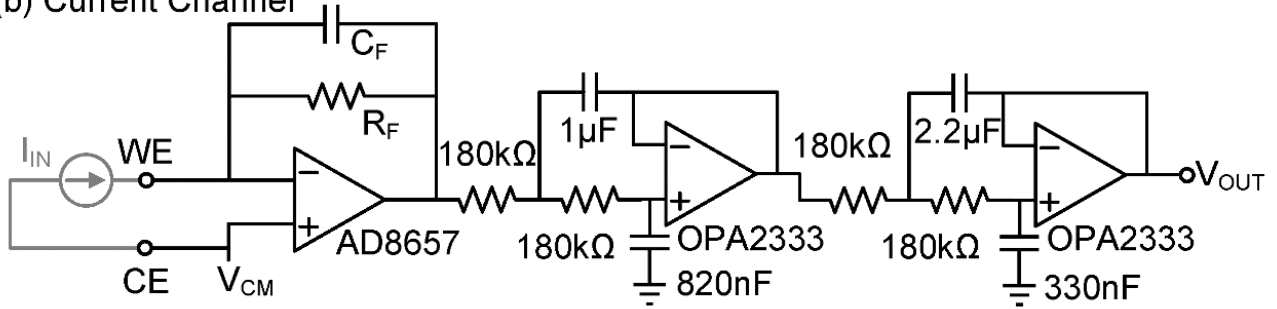


Figure S1: Schematic of the (a) voltage and (b) current sensing channels in the wireless sensor patch.

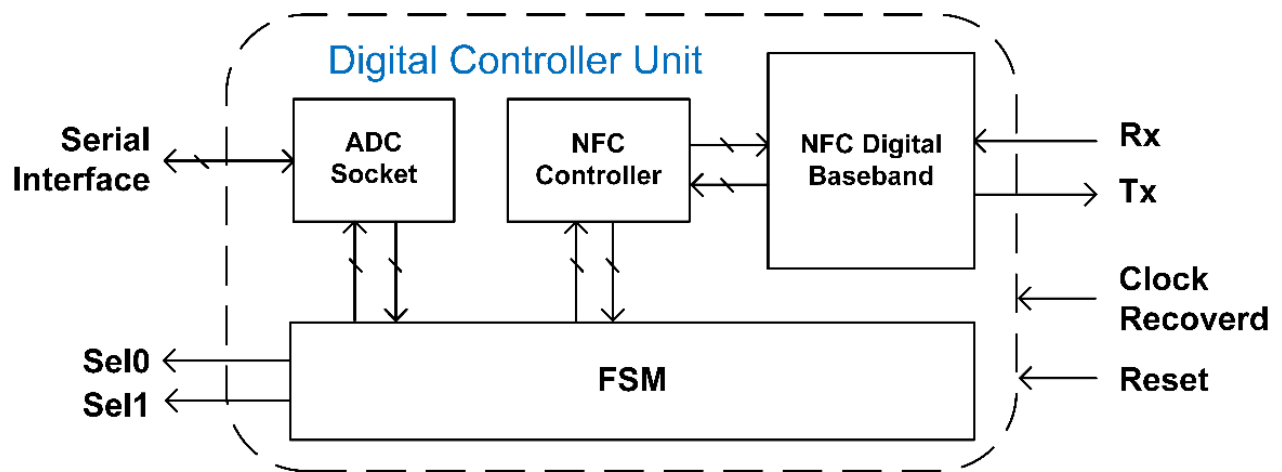


Figure S2: Block diagram of the DCU.

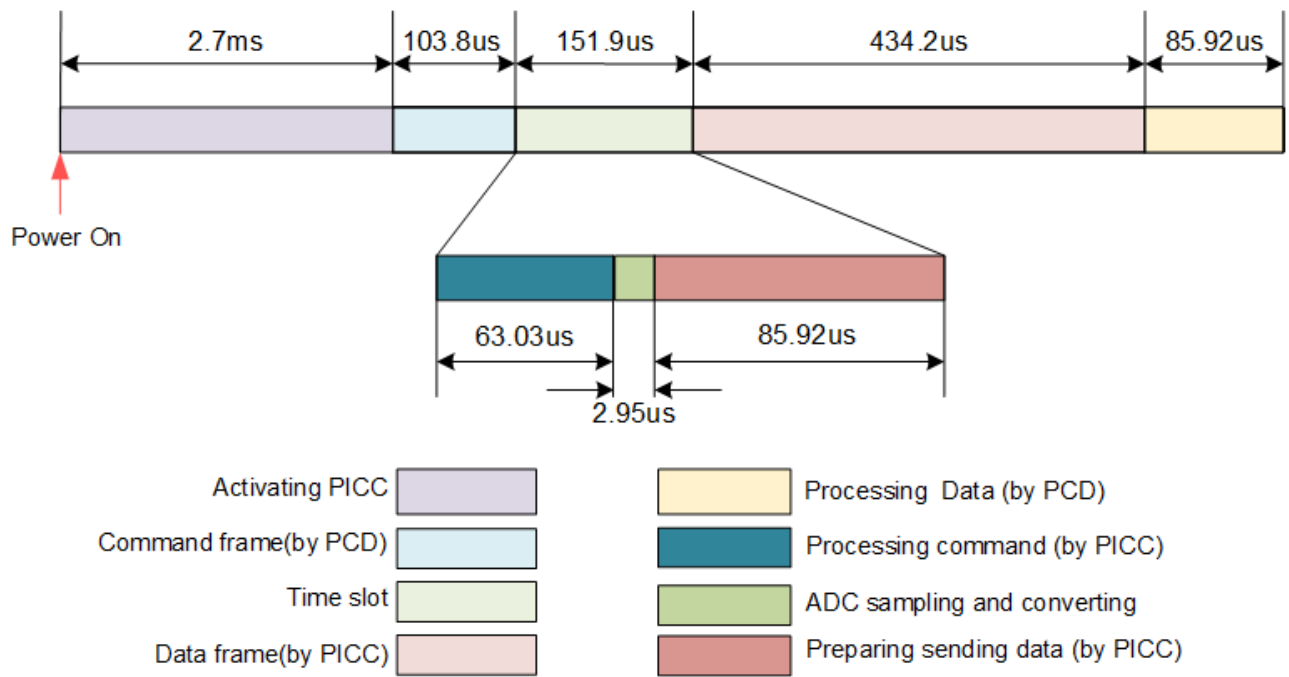


Figure S3: Timing diagram of the working process.

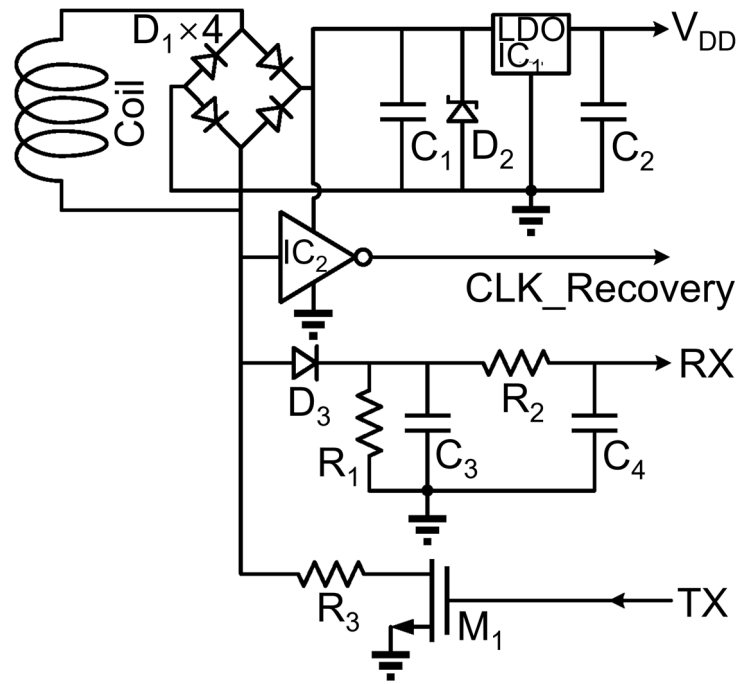


Figure S4: Schematic of the NFC AFE.

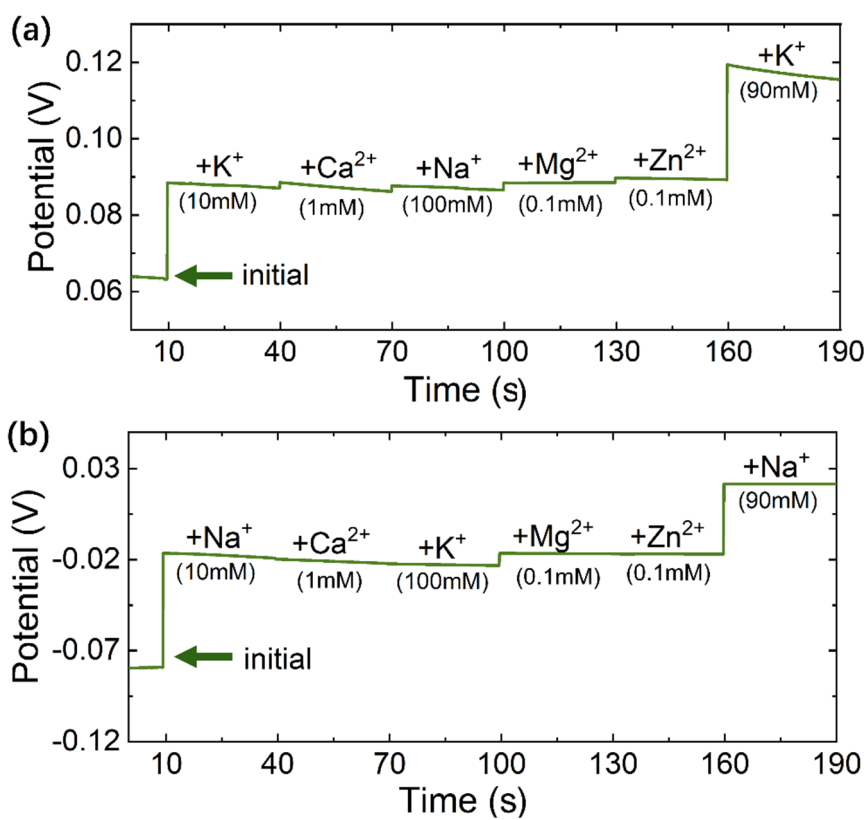


Figure S5: CP curve of ISEs electrode selectivity test results. (a) K⁺ and (b) Na⁺.

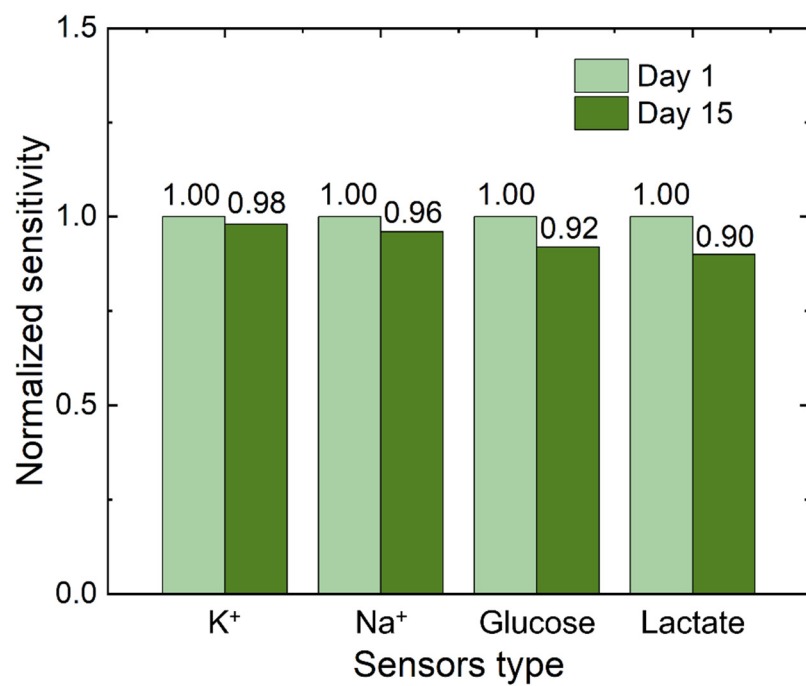


Figure S6: Long-term stability of the sensors.

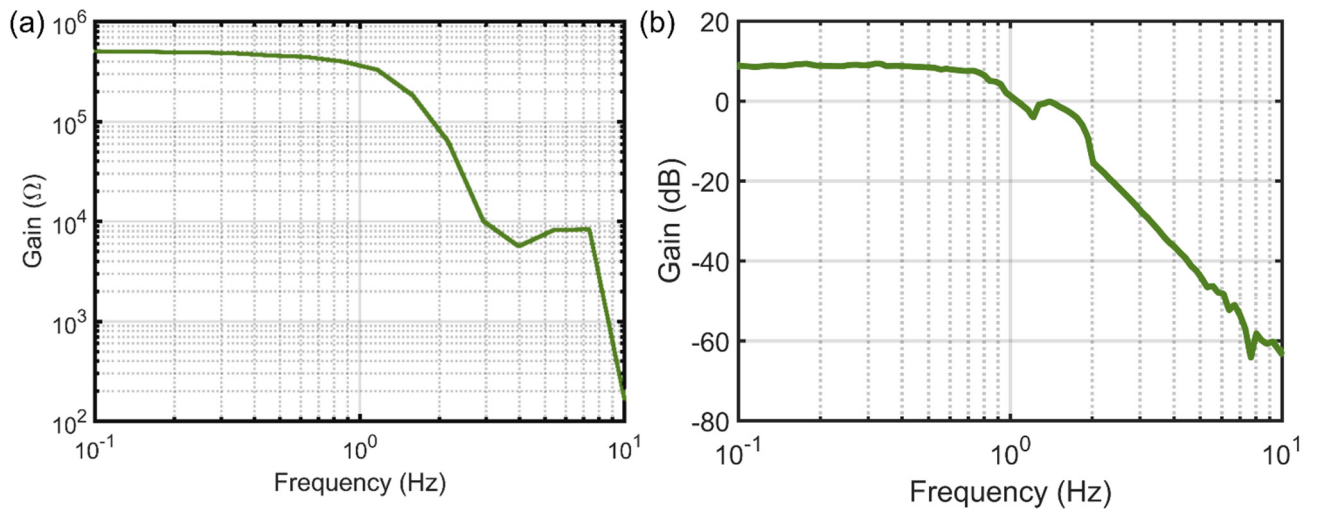


Figure S7: Measured gain-frequency response of the (a) I-mode channel (Transimpedance = 510 k Ω) and (b)

V-mode sensing channel (Gain = 3 V/V).

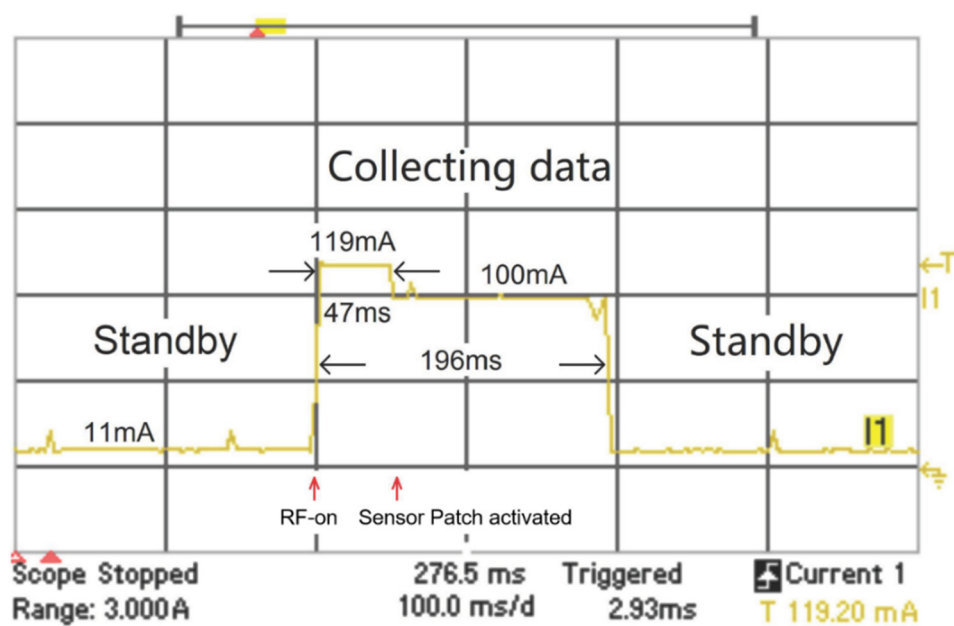


Figure S8: The current waveform of a typical sweat sensing task.

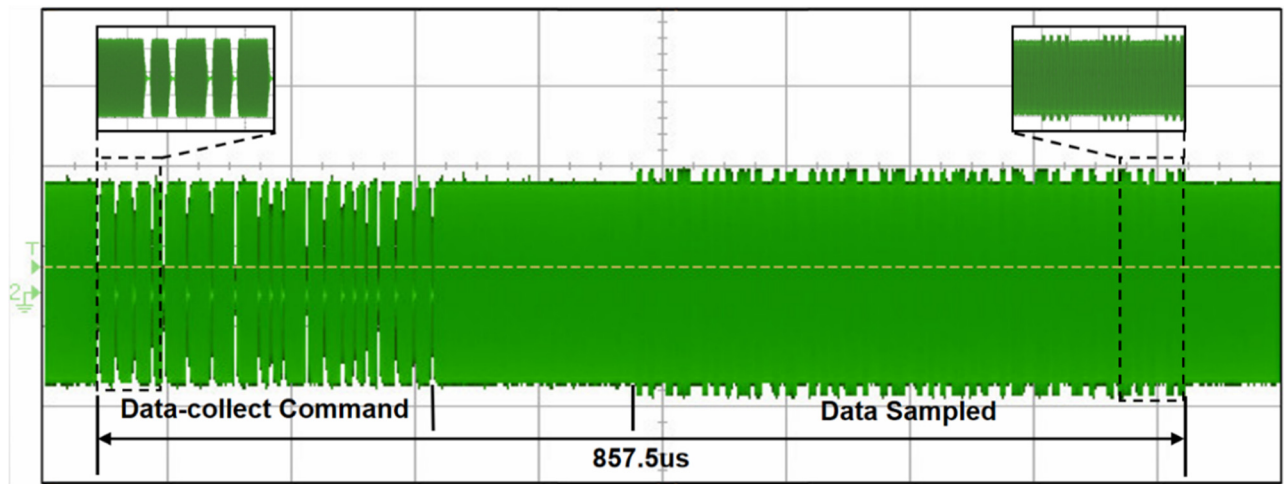


Figure S9: The RF waveform of a typical data collection and transmission task.

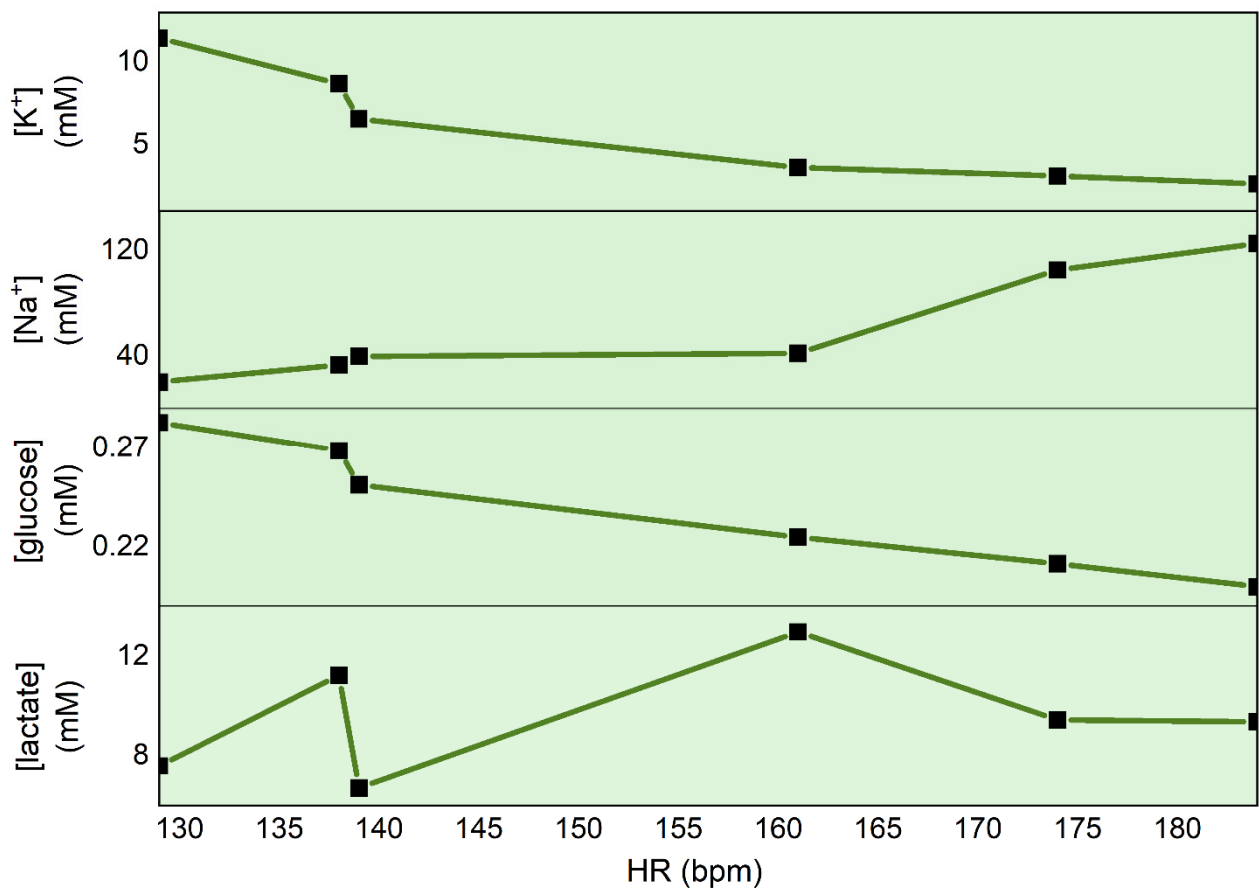


Figure S10: Biosensor responses as a function of HR *ex-vivo* sweat analysis.

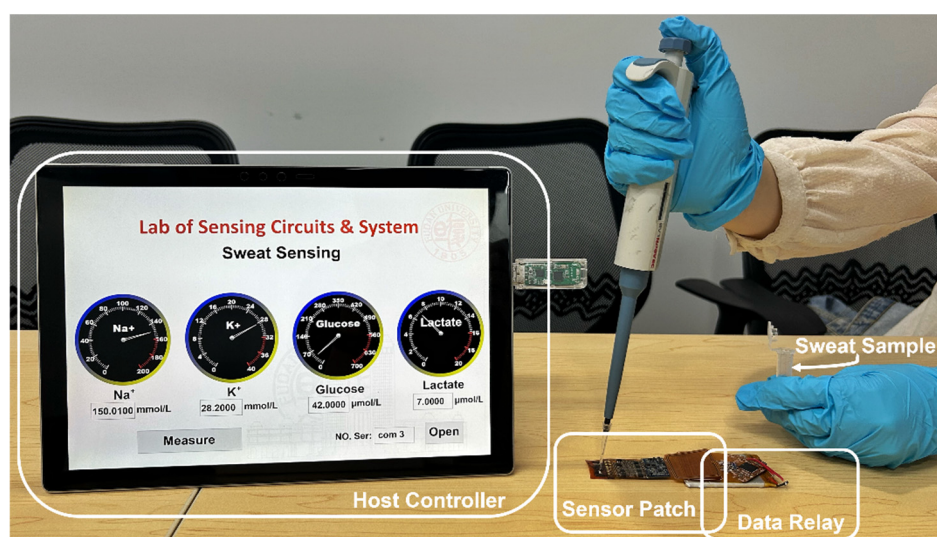


Figure S11: The placement and attachment of the components for the complete system.

Table S1: Key components of the NFC AFE.

Component	Function	Device/Value
D ₁	Rectifier	CUS08F30
C ₁	Decoupling Capacitor	1 μ F, 0402
D ₂	Zener Diode	MMSZ4686
IC ₁	LDO	LP5907-3.3
C ₂	Decoupling Capacitor	1 μ F, 0402
IC ₂	Clock Recovery	SN74LVC1G04DRLR
D ₃	Demodulator	CUS08F30
R ₁	Demodulator	3.6k Ω , 0402
C ₃	Demodulator	43pF, 0402
R ₂	LPF	7.5k Ω , 0402
C ₄	LPF	12pF, 0402
R ₃	Modulator	100 Ω , 0402
M ₁	Modulator	BSS123